

Occurrence of the collective Ziman limit of heat transport in cubic semiconductors: scattering channels and size effects

Jelena Sjakste¹

Maxime Markov¹

Raja Sen¹

Lorenzo Paulatto²

Nathalie Vast¹

E-mail: jelena.sjakste@polytechnique.edu

¹ Laboratoire des Solides Irradiés, CEA/DRF/IRAMIS, Ecole Polytechnique, CNRS, Institut Polytechnique de Paris, F91128 Palaiseau cedex, France

² Sorbonne Université, Museum National d'Histoire Naturelle, UMR CNRS 7590, Institut de Minéralogie, de Physique des Matériaux et de Cosmochimie, 4 place Jussieu, F-75005 Paris, France

Abstract.

In this work, we discuss the possibility of reaching the Ziman conditions for collective heat transport in cubic bulk semiconductors, such as Si, Ge, AlAs and AlP. In natural and enriched silicon and germanium, the collective heat transport limit is impossible to reach due to strong isotopic scattering. However, we show that in hyper-enriched silicon and germanium, as well as in materials with one single stable isotope like AlAs and AlP, at low temperatures, normal scattering plays an important role, making the observation of the collective heat transport possible. We further discuss the effects of sample sizes, and analyse our results for cubic materials by comparing them to bulk bismuth, in which second sound has been detected at cryogenic temperatures. We find that collective heat transport in cubic semiconductors studied in this work is expected to occur at temperatures between 10 and 20 K.

1. Introduction

The study of the heat transport regimes in bulk and low dimensional materials in general, and of the phonon hydrodynamics in particular, currently attracts a renewed interest [1, 2, 3, 4, 5, 6, 7, 8, 9, 10, 11, 12, 13], both from theoretical and experimental viewpoints. The discussion of recent advances can be found in the review article of Ref. [4].

In most of the literature until very recently, a regime in which phonons behave not as independent carriers but as a collective excitation [14, 15] which manifests itself in the form of the second sound temperature wave or of the Poiseuille flow, is referred to as the hydrodynamic regime. Indeed, the hydrodynamic behaviour is expected to occur in the limit where momentum-conserving "normal" phonon-phonon scattering processes dominate over resistive scattering processes. However, it was pointed out recently [2, 3] that this collective Ziman limit is not the only regime in which non-Fourier effects can be observed [3, 6]. As wave-like heat transport at the nanoscale [3, 6] is also referred to as hydrodynamic heat transport in literature [6], and to avoid confusion, in this work we follow the clarification of Ref. [2] and discuss the collective (or Ziman) limit of heat transport, rather than hydrodynamic regime.

The heat flow regimes in suspended graphene and graphene nanoribbons were studied very actively [8, 16, 17, 18, 19, 20, 21] since the prediction, by *ab initio* methods, of the occurrence of collective transport regime in graphene nanoribbons [18, 19, 20, 21]. Recently the Poiseuille flow of phonons was experimentally observed in black phosphorus [9], graphite [22, 1, 7, 23] and SrTiO₃ [24]. All of these materials have particular distinct features in their phonon dispersion facilitating "normal" momentum-conserving scattering processes necessary to reach the collective limit. The first two materials, as well as graphene, belong to the group of 2D- or layered systems in which the non-linear out-of-plane flexural phonon mode plays a role of the efficient scattering channel which accumulates decaying phonons from linear acoustic branches. SrTiO₃ is an "incipient ferroelectric" with a "falling" optical polar phonon mode at the Brillouin zone (BZ) center which strongly decreases in frequency when the temperature is decreased but, in contrast to real ferroelectrics, is eventually stabilized by quantum fluctuations [25, 26]. Moreover, recently coherent second sound waves were observed in a dense magnon gas [27]. At the same time, the collective limit of heat transport was observed only in relatively few "common" 3D materials, such as Bi [28, 29], solid helium [30], and NaF [31, 32] at cryogenic temperatures. In materials such as natural Si and Ge, the dominance of resistive processes, and in particular scattering by isotopes, prevents the occurrence of the collective limit. We note that the importance of the isotopic scattering in the damping of the peak of thermal conductivity at low temperatures was demonstrated in many works [33, 34, 35, 36, 37, 38, 1]. At the same time, we note that in contrast to the collective limit, the "high-frequency", or "driftless" second sound was recently observed in bulk Si and Ge [3, 6] in a rapidly varying temperature field. As it was pointed out in Ref. [3], in the latter case the

dominance of the normal scattering events is not necessary to observe wave-like heat transport, the slow decay of the energy flux being the key requirement instead.

Turning back to the collective limit of heat transport, methods based on the density functional perturbation theory and on the Boltzmann transport equation (BTE) were shown to accurately predict the conditions of the occurrence of the collective limit in many materials [21, 39, 5, 4, 22]. It is expected to occur in samples with sizes defined by the interplay between normal phonon scattering (τ_N), phonon-boundary (τ_b) and resistive scattering (τ_R) times [39], under the condition: $\tau_N < \tau_b < \tau_R$.

In the present work we apply the approach similar to the one of Ref. [39] or Ref. [5] to discuss the conditions of the occurrence of the collective limit of heat transport in cubic semiconductors, such as silicon, germanium, AlAs and AlP, as a function of isotope composition and at temperatures below 50 K. We show that in materials with single stable isotope, such as AlAs and AlP, or in isotopically hyper-enriched silicon, the collective limit of heat transport can be reached at temperatures between 10 and 20 K, where the normal scattering dominates. We show that the reasons for the absence of the collective limit in natural silicon and germanium is isotopic scattering, and that collective heat transport phenomena such as "drifting" second sound could in principle be observed in hyper-enriched silicon and germanium samples, which become available today [40].

2. Methodology and computational details

2.1. Methodology

To identify the conditions for the occurrence of the collective limit of phonon transport, we use the solution of the Boltzmann transport equation (BTE) beyond the single mode approximation (SMA), which allows to explicitly take into account the repopulation of phonon states. Thus, we use a ratio $\kappa_{VAR}/\kappa_{SMA}$ between the lattice thermal conductivity obtained by the solution of BTE and the one obtained with the variational approach (V-BTE) and the one obtained in the single mode approximation (SMA-BTE), as the criterium for the occurrence of the collective regime. We also compare the thermodynamic average scattering rate of "normal" (momentum conserving) phonon-phonon scattering processes, Γ_{av}^n to resistive Umklapp phonon-phonon scattering rate, Γ_{av}^U , as well as to other resistive scattering rates due to isotopic scattering, and to boundary scattering [39]. The thermodynamic averages of different phonon-scattering rates are calculated as [39]: $\Gamma_{av} = \frac{\sum_{\nu} C_{\nu} \Gamma_{\nu}}{\sum_{\nu} C_{\nu}}$, where C_{ν} is the specific heat of the phonon mode ν . We note that in this work, we consider isotropic cubic crystals, in which all transport directions are equivalent, and thus there is no need to consider direction-dependent averages of scattering rates, as it has to be done in highly anisotropic materials [7].

	composition	M_{av}	g_s
HEN	Si ²⁸ -99.9995%, Si ²⁹ -0.0005%	27.98	$6.38 \cdot 10^{-9}$
EN	Si ²⁸ -99.983%, Si ²⁹ -0.014%, Si ³⁰ -0.003%	27.98	$3.31 \cdot 10^{-7}$
NAT	Si ²⁸ -92.23%, Si ²⁹ -4.67%, Si ³⁰ -3.10%	28.09	$2.01 \cdot 10^{-4}$

Table 1. Silicon. Composition, average mass M_{av} (in atomic mass units) and the isotopic disorder parameter g_s for hyper-enriched, HEN, (Ref. [40]), enriched, EN, and natural, NAT, silicon.

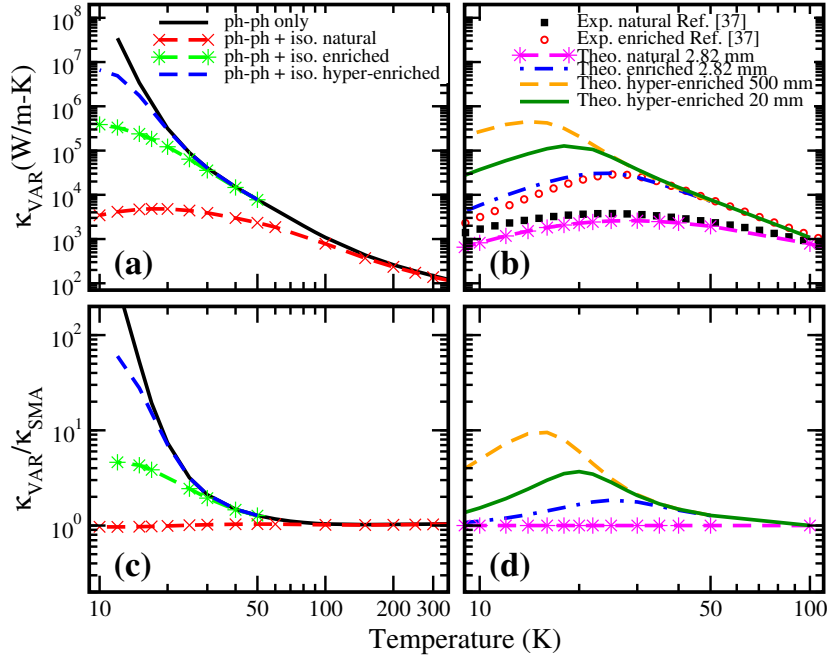


Figure 1. Panels a and c: the lattice thermal conductivity κ_{VAR} and the ratio $\kappa_{VAR}/\kappa_{SMA}$ for Si without boundaries. Black solid line - pure silicon with phonon-phonon scattering mechanism only; Red, blue and green dashed-dotted lines - natural, enriched and hyper-enriched silicon with phonon-phonon + isotopic scattering. Panels c and d: the lattice thermal conductivity and the ratio $\kappa_{VAR}/\kappa_{SMA}$ for Si with boundaries, for different millimetric sample sizes.

2.2. Computational details

Si, AlAs and AlP are described within density functional perturbation theory in local density approximation (DFT-LDA) with norm-conserving pseudopotentials [41]. Harmonic force constants were computed on a $8 \times 8 \times 8$ \mathbf{q} -point grid using Density Functional Perturbation theory (DFPT) [42] as implemented in the QUANTUM ESPRESSO package [43]. Third-order anharmonic constants of the normal and Umklapp phonon interactions have been computed on a $4 \times 4 \times 4$ \mathbf{q} -point grid sampling the Brillouin zone (BZ) using the DFPT formalism as implemented in the D3Q package [44] and then Fourier-interpolated on the denser $30 \times 30 \times 30$ grid necessary for converged integrations of the phonon-phonon scattering rates [44, 45]. The lattice thermal conductivity has been computed with the linearized Boltzmann transport

equation and the variational method (V-BTE) on a $30 \times 30 \times 30$ \mathbf{q} -point grid with the smearing parameter $\sigma = 2 \text{ cm}^{-1}$ [46, 45]. Phonon-boundary scattering is modeled by the Casimir model with the cylindrical geometry for millimeter-sized wires [47, 45, 48], in the completely diffusive limit with no specularity [39, 49]. Isotope scattering is described with the widely used Tamura model [50, 51, 47, 45] with the scattering probability:

$$P_{j\mathbf{q},j'\mathbf{q}'}^{iso} = \frac{\pi}{2N_0} \omega_{j\mathbf{q}} \omega_{j'\mathbf{q}'} \left[n_{j\mathbf{q}} n_{j'\mathbf{q}'} + \frac{n_{j\mathbf{q}} + n_{j'\mathbf{q}'}}{2} \right] \times \\ \times \delta(\hbar\omega_{j\mathbf{q}} - \hbar\omega_{j'\mathbf{q}'}) \sum_s g_s \left| \sum_{\alpha} z_{j\mathbf{q}}^{s\alpha} * z_{j'\mathbf{q}'}^{s\alpha} \right|^2 \quad (1)$$

where s run over all atoms, α is the Cartesian coordinate index, j is the phonon branch index, \mathbf{q} is the phonon wavevector, $z_{j\mathbf{q}}^{s\alpha}$ is the phonon eigenmode, $\omega_{j\mathbf{q}}$ is the phonon frequency, $g_s = \frac{(M_s - \langle M_s \rangle)^2}{\langle M_s \rangle}$ is the mass variance parameter.

3. Results: calculated thermal conductivity

3.1. Phonon state repopulation in Si and isotope scattering effect

In panel a of figure 1, we show the thermal conductivity (without boundary) calculated within the V-BTE approach for natural silicon, isotopically enriched silicon, and extra-pure silicon which became available recently [40], and which we will refer to as "hyper-enriched Si" in the present work. The isotopic compositions of Si studied in our work are summarized in table 1. In panel b, we show our results for the thermal conductivity of silicon in presence of boundary scattering. In presence of boundary scattering, our calculated thermal conductivity of Si with various isotopic compositions is found in good agreement with available experimental data [37, 38]. We note that our calculations of the lattice thermal conductivity of Si, as well as those of AlAs and AlP which will be discussed later, are also in agreement with previous *ab initio* calculations [52, 53] (previous theoretical data of Ref. [53] has been obtained for the 100-400 K temperature range).

In panel c of Fig. 1, we show the ratio $\kappa_{VAR}/\kappa_{SMA}$, for Si with various isotopic compositions. At room temperatures and down to 70 K, the ratio $\kappa_{VAR}/\kappa_{SMA}$ is equal to one for all samples, which is a clear signature of the kinetic regime, where heat is transported by single phonon modes. However, as one can see in panel c, the ratio $\kappa_{VAR}/\kappa_{SMA}$ for isotopically pure silicon attains two orders of magnitude below 20 K (black curve), and similar results are obtained for hyper-enriched silicon (blue dashed curve), demonstrating the importance of the normal processes and of the repopulation for pure and hyper-enriched samples below 20 K. Therefore, the possibility of the collective heat transport limit is not excluded for these samples. In contrast, one can see that the collective heat transport limit is not possible in natural silicon according to our analysis (red dashed curve with crosses), and in agreement with common knowlege. Indeed, the $\kappa_{VAR}/\kappa_{SMA}$ ratio is close to one, and thus one can

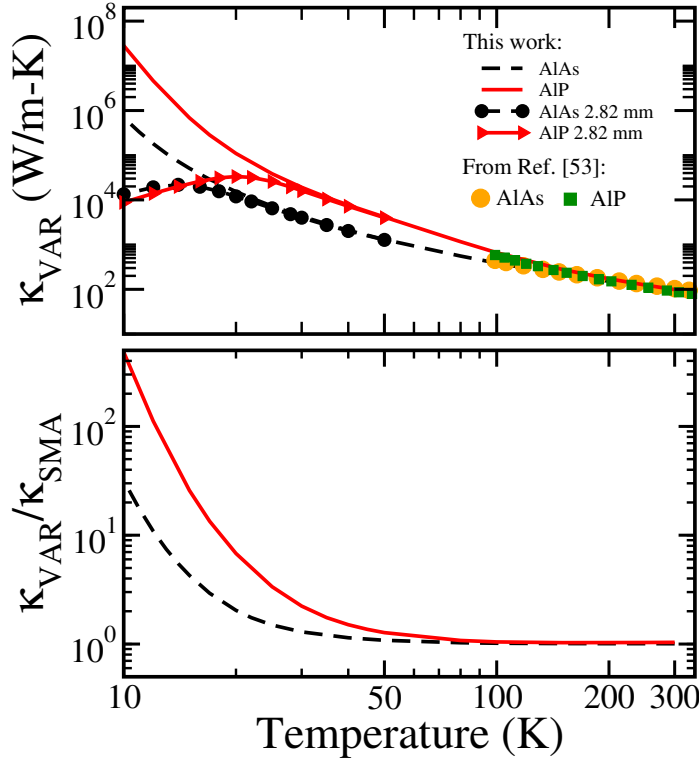


Figure 2. Panels a and b: the lattice thermal conductivity κ_{VAR} and the ratio $\kappa_{VAR}/\kappa_{SMA}$ for AlP and AlAs. Black solid and dashed lines - pure AlP and AlAs respectively with phonon-phonon interaction only.

conclude that the resistive processes dominate and that the repopulation does not play any important role in the latter case. In the isotopically enriched silicon case (green dashed curve with dots), the $\kappa_{VAR}/\kappa_{SMA}$ ratio is much larger than that of the natural silicon, however, there is no temperature regime in which it attains one order of magnitude.

According to our results, the same conclusions are valid for germanium (results not shown): in natural and isotopically enriched samples, the possibility of the collective heat transport limit which could potentially exist in hyper-enriched or pure samples, is destroyed by isotopic scattering.

In order to further investigate the possibility of the collective heat transport limit in the isotopically hyper-enriched silicon and to compare with experiments, we include boundary scattering. In panels b and d of Fig. 1, we show the thermal conductivity of Si and the ratio $\kappa_{VAR}/\kappa_{SMA}$ for various isotopic compositions and in presence of boundary scattering for different sample sizes. In panel b, our computational results for 2.82 mm sample size, for natural and enriched silicon, are compared with the experimental results of Ref. [37]. As one can see, the agreement between calculated and experimental thermal conductivity is very good. To illustrate the effect of sample size on the lattice thermal conductivity, we also show the calculated results in hyper-enriched silicon for the 20 mm and 500 mm sizes.

As one can see in panel d of Fig. 1, as expected, the ratio $\kappa_{VAR}/\kappa_{SMA}$ is reduced in presence of the boundary scattering, for all sizes and all isotopic compositions. Nevertheless, normal processes play an important role for hyper-enriched samples, especially for sample sizes of 20 mm and larger.

The possibility of the collective heat transport limit in isotopically enriched samples of 2.82 mm size was discussed in Ref. [37]. As one can see in panel d of Fig. 1, we find indeed that the ratio $\kappa_{VAR}/\kappa_{SMA}$ for those samples (blue dot-dashed curve) exceeds 1 for temperatures between 10 K and 60 K, with the maximum value of 1.8 at 25 K, confirming the conclusions of Ref. [37] that the collective heat transport can exist to some extent. However, the effect of the repopulation of phonon states by the normal processes is strongly reduced by the isotopic and boundary scattering for 2.82 mm samples.

3.2. Repopulation in AlAs and AlP

In the previous section, we have demonstrated that the isotopic scattering is the main reason why the collective limit can not be observed in Si and Ge, while it could exist in pure or hyper-enriched samples. This is the reason why we have decided to further explore cubic materials that naturally have no isotopes, such as AlP and AlAs.

In panel a of Fig. 2, we show our calculated lattice thermal conductivity for AlP and AlAs, as a function of temperature. In panel b of Fig. 2, in analogy with the analysis of Fig. 1, we show the ratio $\kappa_{VAR}/\kappa_{SMA}$ for AlP and AlAs. One can see that, similarly to pure Si, the $\kappa_{VAR}/\kappa_{SMA}$ ratio for AlP attains two orders of magnitude around 17 K. The same is true for AlAs, at slightly lower temperatures around 8 K. Thus, we conclude that according to our results, repopulation due to normal processes is very strong in AlP and AlAs at low temperatures. Therefore, the collective transport limit can also exist in AlP and AlAs. Also, we can conclude that contrary to common belief, normal processes play an important role in cubic materials such as Si, AlP and AlAs, but at temperatures below 20 K, and when isotopic scattering is absent or strongly reduced. In the next section, we further analyse the effect of sample sizes.

4. Discussion: size effects and scattering rates

The effect of boundary scattering, analysed in panel d of Fig. 1 for silicon, appears to be very strong. Indeed, the $\kappa_{VAR}/\kappa_{SMA}$ between 10 and 20 K for hyper-enriched samples is reduced by almost two orders of magnitude (without borders), from about one hundred to 3.7 in 20 mm samples (green curve).

In Fig. 3, we compare $\kappa_{VAR}/\kappa_{SMA}$ ratios in hyper-enriched silicon, cubic AlP and bismuth, which was studied in our earlier works [39, 48]. The interest in comparing materials studied in the present work with Bi resides in the fact that the collective heat transport (drifting second sound) was experimentally observed in the latter [28]. As one can see in Fig. 3, scattering by boundaries reduces the repopulation effects

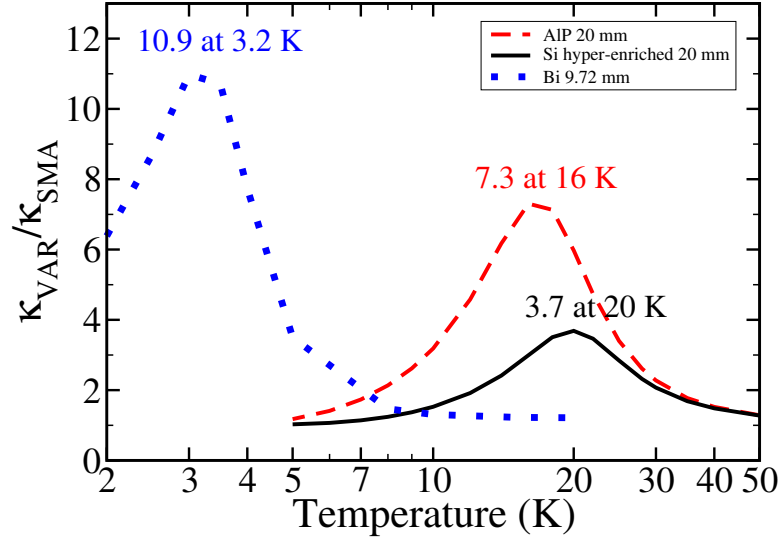


Figure 3. $\kappa_{VAR}/\kappa_{SMA}$ ratio for AIP and hyper-enriched Si samples of 20 mm, compared to $\kappa_{VAR}/\kappa_{SMA}$ ratio for Bi sample of 9.72 mm.

in all three materials. We can also note that the effect of repopulation reduction by boundary scattering appears to be somewhat weaker in Bi, resulting in a larger peak value of $\kappa_{VAR}/\kappa_{SMA}$ ratio. At the same time, the peak value of $\kappa_{VAR}/\kappa_{SMA}$ in AIP at 16 K for 20 mm sample is still comparable to that of Bi at 3.2 K for 9.72 mm sample, indicating that observation of the collective heat transport limit in AIP must be possible at temperatures around 16 K for 20 mm samples.

To further understand why the effect of repopulation reduction by boundary scattering is stronger in Si and AIP compared to Bi, we study the average scattering rates in Fig. 4. By comparing the Umklapp and normal scattering rates in panels a (Si), b (AIP) and c (Bi) of Fig. 4, we notice that overall, in all three materials the normal scattering dominates over the Umklapp scattering at low temperatures. In that respect, cubic materials studied in this work are similar to Bi. The major role of isotopic scattering, which is the dominant scattering process below 70 K in natural silicon, is also illustrated in panel a of Fig. 4.

Coming now to boundary scattering rates, we notice that for equal sample sizes, boundary scattering rates are 4 to 5 times larger in Si and AIP, compared to Bi. This fact, which is due to larger phonon group velocities in Si and AIP as compared to those in Bi, explains why the repopulation reduction by boundary scattering is stronger in Si and AIP.

5. Conclusions

In this work we have performed the theoretical analysis of the conditions necessary to reach the collective heat transport limit in silicon with various isotopic compositions, as well as in AlAs and AIP which contain naturally one single stable isotope. While the

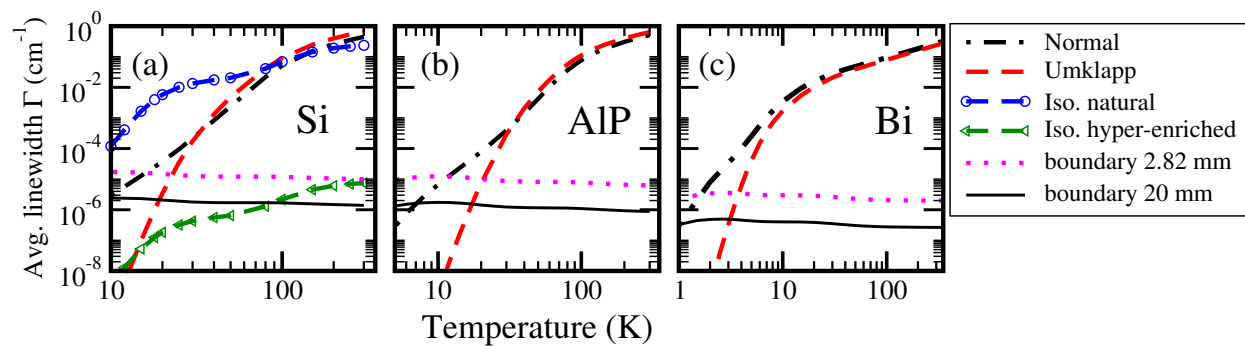


Figure 4. The thermodynamic average of phonon linewidth. Black dot-dashed lines - normal processes, red dashed line - Umklapp processes; blue and green lines with symbols - isotopic scattering for natural and hyper-enriched silicon. Horizontal lines: boundary scattering for 2.82 mm (red dotted line) and 20 mm (black solid line) samples.

collective heat transport is impossible in natural silicon due to isotopic scattering, it can in principle be reached in hyper-enriched Si, as well as in natural AlAs and AlP. We have shown that, contrarily to common belief, the normal phonon-phonon scattering processes play an important role in cubic semiconductors below 20 K, similarly to Bi where collective heat transport phenomena have been experimentally observed. In addition, in the cubic materials studied in this work, the possibility to reach the collective heat transport limit is reduced by the large phonon group velocities that enhance the effect of boundary scattering with respect to, e.g., bismuth. Nevertheless, as we have shown in the present work, the observation of the collective heat transport limit in AlP must be possible at temperatures around 16 K for 20 mm samples.

6. Acknowledgements

Calculations have been performed with the Quantum ESPRESSO computational package [43] and the D3Q code [44, 45]. We are grateful to A.V. Inyushkin for providing the experimental data published in Refs. [37, 38]. We acknowledge useful discussions with B. Fauquet and F. Mauri. This work has been granted access to HPC resources by the French HPC centers GENCI-IDRIS, GENCI-CINES and GENCI-TGCC (Project 2210) and by the Ecole Polytechnique through the *Three Lab Computing* cluster. Financial support from the ANR PLACHO project ANR-21-CE50-0008 is gratefully acknowledged.

- [1] Z. Ding, K. Chen, B. Song, J. Shin, A. Maznev, K. Nelson, and G. Chen. Observation of second sound in graphite over 200 K. *Nat. Comm.*, 13:285, 2022.
- [2] L. Sendra, A. Beardo, J. Bafaluy, P. Torres, F. X. Alvarez, and J. Camacho. Hydrodynamic heat transport in dielectric crystals in the collective limit and the drifting/driftless velocity conundrum. *Phys. Rev. B*, 106:155301, 2022.
- [3] A. Beardo, M. López-Suárez, L. A. Pérez, L. Sendra and M. I. Alonso, C. Melis, J. Bafaluy,

- J. Camacho, L. Colombo, R. Rurali, F. X. Alvarez, and J. S. Reparaz. Observation of second sound in a rapidly varying temperature field in Ge. *Sci. Adv.*, 7:eabg4677, 2021.
- [4] K. Ghosh, A. Kusiak, and J.-L. Battaglia. Phonon hydrodynamics in crystalline materials. *J. Phys.: Condens. Matter*, 34:323001, 2022.
- [5] K. Ghosh, A. Kusiak, and J.-L. Battaglia. Effect of characteristic size on the collective phonon transport in crystalline GeTe. *Phys. Rev. Materials*, 5:073605, 2021.
- [6] A. Beardo, M. Calvo-Schwarzwalder, J. Camacho, T. G. Myers, P. Torres, L. Sendra, F. X. Alvarez, and J. Bafaluy. Hydrodynamic heat transport in compact and holey silicon thin films. *Phys. Rev. App.*, 11:034003, 2019.
- [7] Z. Ding, J. Zhou, B. Song, V. Chiloyan, M. Li, T.-H. Liu, and G. Chen. Phonon hydrodynamic heat conduction and knudsen minimum in graphite. *Nano Lett.*, 18:638, 2018.
- [8] Y. Machida¹, N. Matsumoto, T. Isono, and K. Behnia. Phonon hydrodynamics and ultrahigh-room-temperature thermal conductivity in thin graphite. *Science*, 367:309, 2020.
- [9] Y. Machida, A. Subedi, K. Akiba, A. Miyake, M. Tokunaga, Y. Akahama, K. Izawa, and K. Behnia. Observation of Poiseuille flow of phonons in black phosphorus. *Science Advances*, 4:eaat3374, 2018.
- [10] D. G. Cahill, P. V. Braun, G. Chen, D. R. Clarke, S. H. Fan, K. E. Goodson, P. Keblinski, W. P. King, G. D. Mahan, A. Majumdar, H. J. Maris, S. R. Phillpot, E. Pop, and L. Shi. Nanoscale thermal transport. II. 2003-2012. *Applied Physics Reviews*, 1:011305, 2015.
- [11] S. Volz, J. Ordonez-Miranda, A. Shchepetov, M. Prunnila, J. Ahopelto, T. Pezeril, G. Vaudel, V. Gusev, P. Ruello, E. Weig, M. Schubert, M. Hettich, M. Grossman, T. Dekorsy, F. Alzina, B. Graczykowski, E. Chavez-Angel, J.-S. Reparaz, M. R. Wagner, C. M. Sotomayor-Torres, S. Xiong, S. Neogi, and D. Donadio. Nanophononics: state of the art and perspectives. *Eur. Phys. J. B*, 89:15, 2016.
- [12] C. W. Chang, D. Cohen Okawa, H. Garcia, A. Majumdar, and A. Zettl. Breakdown of Fourier’s law in nanotube thermal conductors. *Phys. Rev. Lett.*, 101:075903, 2008.
- [13] N. Yand, G. Zhang, and B. Li. Violation of Fourier’s law and anomalous heat diffusion in silicon nanowires. *Nano Today*, 5:85, 2010.
- [14] A. Cepellotti and N. Marzari. Thermal transport in crystals as a kinetic theory of relaxons. *Phys. Rev. X*, 6:041013, 2016.
- [15] A. Cepellotti and N. Marzari. Transport waves as crystal excitations. *Phys. Rev. Mat.*, 1:045406, 2017.
- [16] X. Li and S. Lee. Crossover of ballistic, hydrodynamic, and diffusive phonon transport in suspended graphene. *Phys. Rev. B*, 99:085202, 2019.
- [17] A. K. Majee and Z. Aksamija. Dynamical thermal conductivity of suspended graphene ribbons in the hydrodynamic regime. *Phys. Rev. B*, 98:024303, 2018.
- [18] J. Zhang, X. Huang, Y. Yue, J. Wang, and X. Wang. Dynamical response of graphene to thermal impulse. *Phys. Rev. B*, 84:235416, 2011.
- [19] G. Fugallo, A. Cepellotti, L. Paulatto, M. Lazzeri, N. Marzari, and F. Mauri. Thermal conductivity of graphene and graphite: collective excitations and mean free paths. *Nano Lett.*, 14:6109, 2014.
- [20] S. Lee, D. Broido, K. Esfarjani, and G. Chen. Hydrodynamic phonon transport in suspended graphene. *Nature Communications*, 6:6290, 2015.
- [21] A. Cepellotti, G. Fugallo, L. Paulatto, M. Lazzeri, F. Mauri, and N. Marzari. Phonon hydrodynamics in two-dimensional materials. *Nature Communications*, 6:6400, 2015.
- [22] X. Huang, Y. Guo, Y. Wu, S. Masubuchi, K. Watanabe, T. Taniguchi, Z. Zhang, S. Volz, T. Machida, and M. Nomura. Observation of phonon Poiseuille flow in isotopically purified graphite ribbons. *Nat. Comm.*, 14:2044, 2023.
- [23] S. Huberman, R.A. Duncan, K. Chen, B. Song, V. Chiloyan, Z. Ding, A.A. Maznev, G. Chen, and K.A. Nelson. Observation of second sound in graphite at temperatures above 100 K. *Science*, 10.1112:science.aav3548, 2019.
- [24] V. Martelli, J.L. Jimenez, M. Continentino, E. Baggio-Saitovitch, and K. Behnia. Thermal

- transport and phonon hydrodynamics in strontium titanate. *Phys. Rev. Lett.*, 120:125901, 2018.
- [25] K. M. Rabe, C. H. Ahn, and J.-M. Triscone. *Physics of Ferroelectrics. A Modern Perspective*. Springer-Verlag, Berlin Heidelberg, 2007.
- [26] V. L. Gurevich and A. K. Tagantsev. Second sound in ferroelectrics. *Sov. Phys. JETP*, 67:206–212, 1988.
- [27] V. Tiberkevich, I. V. Borisenko, P. Nowik-Boltyk, V. E. Demidov, A. B. Rinkevich, S. O. Demokritov, and A. N. Slavin. Excitation of coherent second sound waves in a dense magnon gas. *Scientific Reports*, 9:9063, 2019.
- [28] V. Narayanamurti and R.C. Dynes. Observation of second sound in bismuth. *Phys. Rev. Lett.*, 28:1461, 1972.
- [29] L.P. Mezhov-Deglin, V.N. Kopylov, and E.S. Medvedev. Contributions of various phonon relaxation mechanisms to the thermal resistance of the crystal lattice of bismuth at temperatures below 2 K. *Sov. Phys. JETP*, 40:557, 1974.
- [30] C. C. Ackerman, B. Bertman, H. A. Fairbank, and R. A. Guyer. Second sound in solid helium. *Phys. Rev. Lett.*, 16:789, 1966.
- [31] H. E. Jackson, C. T. Walker, and T. F. McNelly. Second sound in NaF. *Phys. Rev. Lett.*, 25:26, 1970.
- [32] D. W. Pohl and V. Irniger. Observation of Second Sound in NaF by Means of Light Scattering. *Phys. Rev. Lett.*, 36:480, 1976.
- [33] P. D. Thacher. Effect of boundaries and isotopes on thermal conductivity of LiF. *Phys. Rev.*, 156:975, 1967.
- [34] V. I. Ozhogin, A. V. Inyushkin, A. N. Taldenkov, A. V. Tikhomirov, and G. E. Popov. Isotope effect in the thermal conductivity of germanium single crystals. *JETP Lett.*, 63:490, 1996.
- [35] A. P. Zhernov and A. V. Inyushkin. Kinetic coefficients in isotopically disordered crystals. *Phys. Usp.*, 45:527–555, 2002.
- [36] L. Lindsay. First principles Peierls-Boltzmann phonon thermal transport: A topical review. *Nanoscale and Microscale Thermophysical Engineering*, 20:67, 2016.
- [37] A. V. Inyushkin, A. N. Taldenkov, A. M. Gibin, A. V. Gusev, and H.-J. Pohl. On the isotope effect in thermal conductivity of silicon. *Phys. Status Solidi C*, 1:2995, 2004.
- [38] A. V. Inyushkin, N. V. Abrosimov, A. N. Taldenkov, J. W. Ager, E. E. Haller, H. Riemann, H.-J. Pohl, and P. Becker. Ultrahigh thermal conductivity of isotopically enriched silicon. *J. Appl. Phys.*, 123:095112, 2018.
- [39] M. Markov, J. Sjakste, G. Barbarino, G. Fugallo, L. Paulatto, M. Lazzeri, F. Mauri, and N. Vast. Hydrodynamic heat transport regime in bismuth : a theoretical viewpoint. *Phys. Rev. Lett.*, 120:075901, 2018.
- [40] N.V. Abrosimov, D.G. Aref'ev, P. Becker, H. Bettin, A.D. Bulanov, M. F. Churbanov, S.V. Filimonov, V.A. Gavva, O.N. Godisov, A.V. Gusev, T.V. Kotereva, D. Nietzold, M. Peters, A.M. Potapov, H.-J. Pohl, A. Pramann, H. Riemann, P.-T. Scheel, R. Stosch, S. Wundrack, and S. Zakel. A new generation of 99.999 enriched 28 Si single crystals for the determination of Avogadro's constant. *Metrologia*, 54:599, 2017.
- [41] M. Fuchs and *et al.* <http://www.fhi-berlin.mpg.de/th/fhi98md/fhi98PP/>.
- [42] S. Baroni, S. de Gironcoli, A. Dal Corso, and P. Giannozzi. Phonons and related crystal properties from density-functional perturbation theory. *Rev. Mod. Phys.*, 73:515, 2001.
- [43] P. Giannozzi, O. Andreussi, T. Brumme, O. Bunau, M. Buongiorno Nardelli, M. Calandra, R. Car, C. Cavazzoni, D. Ceresoli, M. Cococcioni, N. Colonna, I. Carnimeo, A. Dal Corso, S. de Gironcoli, P. Delugas, R. A. DiStasio Jr. and A. Ferretti, A. Floris, G. Fratesi, G. Fugallo, R. Gebauer, U. Gerstmann, F. Giustino, T. Gorni, J. Jia, M. Kawamura, H.-Y. Ko, A. Kokalj, E. Küçükbenli, M. Lazzeri, M. Marsili, N. Marzari, F. Mauri, N. L. Nguyen, H.-V. Nguyen, A. Otero de-la Roza, L. Paulatto, S. Poncé, D. Rocca, R. Sabatini, B. Santra, M. Schlipf, A. P. Seitsonen, A. Smogunov, I. Timrov, T. Thonhauser, P. Umari, N. Vast, X. Wu, and S. Baroni.

- Advanced capabilities for materials modelling with QUANTUM ESPRESSO. J. Phys.: Condens. Matter, 29:465901, 2017.
- [44] L. Paulatto, F. Mauri, and M. Lazzeri. Anharmonic properties from a generalized third-order *ab initio* approach: Theory and applications to graphite and graphene. Phys. Rev. B, 87:214303, 2013.
- [45] G. Fugallo, M. Lazzeri, L. Paulatto, and F. Mauri. *Ab initio* variational approach for evaluating lattice thermal conductivity. Phys. Rev. B, 88:045430, 2013.
- [46] M. Omini and A. Sparavigna. An iterative approach to the phonon Boltzmann equation in the theory of thermal conductivity. Physica B, 212:101, 1995.
- [47] A. Sparavigna. Influence of isotope scattering on the thermal conductivity of diamond. Phys. Rev. B, 65:064305, 2002.
- [48] M. Markov, J. Sjakste, G. Fugallo, L. Paulatto, M. Lazzeri, F. Mauri, and N. Vast. Nanoscale mechanisms for the reduction of heat transport in bismuth. Phys. Rev. B, 93:064301, 2016.
- [49] R. Sen, N. Vast, and J. Sjakste. Role of dimensionality and size in controlling the drag seebeck coefficient of doped silicon nanostructures: A fundamental understanding. Phys. Rev. B, 108:L060301, 2023.
- [50] S. Tamura. Isotope scattering of dispersive phonons in Ge. Phys. Re. B, 27:858, 1983.
- [51] M. Omini and A. Sparavigna. Heat transport in dielectric solids with diamond structure. Il Nuovo Cimento D, 19:1537, 1997.
- [52] A. Ward, D. A. Broido, D. A. Stewart, and G. Deinzer. *Ab initio* theory of the lattice thermal conductivity in diamond. Phys. Rev. B, 80:125203, 2009.
- [53] L. Lindsay, D. A. Broido, and T. L. Reinecke. *Ab initio* thermal transport in compound semiconductors. Phys. Rev. B, 87:165201, 2013.